



# Structure-based design, synthesis, biological evaluation, and molecular docking of novel 10-methoxy dibenzo[b,h][1,6]naphthyridinecarboxamides

K. N. Vennila<sup>1</sup> · B. Selvakumar<sup>2</sup> · V. Satish<sup>2</sup> · D. Sunny<sup>3</sup> · S. Madhuri<sup>3</sup> · K. P. Elango <sup>1</sup>

Received: 3 July 2020 / Accepted: 29 September 2020  
© Springer Science+Business Media, LLC, part of Springer Nature 2020

## Abstract

10-methoxy dibenzo[b,h][1,6]naphthyridine carboxylic acid was successfully synthesized from 3-methoxyaniline by a new route. By utilizing a structure-based epharmacophore developed from the active site of 3-phosphoinositide-dependent kinase-1, a series of nine novel 10-methoxy dibenzo[b,h][1,6]naphthyridinecarboxamides was synthesized and characterized by different spectral techniques. Three of them are found to be active by screening against A549 cell line and showed significant anticancer activity when compared to a marketed lung cancer drug, pemetrexed. The molecular docking and in silico pharmacokinetic predictions provide detailed understanding for utilizing the dibenzo[b,h][1,6]naphthyridine scaffold in future drug discovery and development of PDK1 inhibitors.

**Keywords** Dibenzonaphthyridines · Phosphoinositide-dependent kinase · Epharmacophore · Pharmacophore modeling · ATP site · Molecular docking

## Introduction

Fused heterocycles always attract chemists due to their broad spectrum of biological applications. Naphthyridine is one such fused bicyclic nitrogen containing a heterocycle reported to show a lot of pharmacological and biological activities. There are many literature examples of [1,8]naphthyridine synthesis, antibacterial, and anticancer activity [1]. Nalidixic acid, a marketed [1,8]naphthyridine analog, is more effective against both Gram-positive and Gram-negative bacteria [2]. Malaridine phosphate is another well-known antimalarial drug, and vosaroxin is the one that is undergoing phase III clinical

trials for acute myeloid leukemia [3]. Like this, [1,6]naphthyridine has been shown to be a prominent scaffold with drug-like properties [4, 5]. There are several reports on the synthesis and biological activities of naphthyridines, but only a few are on dibenzo[1,6]naphthyridines [6–9]. Hence, several efforts have been made to efficiently synthesize dibenzonaphthyridines. These compounds are also reported as important with significant biological activities in vitro, such as 3-phosphoinositide-dependent kinase-1 inhibition [10, 11], topoisomerase I inhibition [12], DNA-intercalating agents [13], antimalarials, and anticancer agents [14, 15]. Recently, it was displayed that 8-substituted-[1,6] naphthyridines exhibit HIV-1 integrase inhibitory activity and cytotoxicity against cancer cells [4]. Thus, the dibenzo[b,h][1,6]naphthyridines can also be potentially developed as anticancer drugs by structural modification and examining their in vitro activity. Furthermore, these compounds are known for their fluorescence properties and found application in fluorescent DNA detection and quantification [16–18]. Also, it can be said that this particular scaffold gained more attention only in recent years and has not been explored much. Only a limited number of reports dealing with the synthetic methods of [1,6]dibenzonaphthyridine class of compounds are available [19]. The synthesis of dibenzo[b,h][1,6]naphthyridines is found in a few recent reports in which we find CuBr<sub>2</sub>-catalyzed reaction [20],

**Supplementary information** The online version of this article (<https://doi.org/10.1007/s00044-020-02645-x>) contains supplementary material, which is available to authorized users.

✉ K. P. Elango  
drkpelango@rediffmail.com

<sup>1</sup> Department of Chemistry, Gandhigram Rural Institute (Deemed to be University), Gandhigram 624302, India

<sup>2</sup> Anthem Biosciences Private Limited, Bengaluru 560099, India

<sup>3</sup> National Institute of Animal Biotechnology, Hyderabad 500049, India

palladium ligand-free catalyzed reaction [21], iodine-catalyzed reaction [2], one-pot synthesis [16], and Sc(OTf)<sub>3</sub>-catalyzed cascade approach [17]. These results prompted us to look into the ways of synthesizing novel 10-methoxy dibenzo[b,h][1,6]naphthyridine derivatives from easily available reagents and with their reductive amination.

Also, Pi3K/AKT/mTOR is a well-known pathway in cancer cell signaling, and there are numerous reports mentioning that its inhibition could potentially provide valuable therapeutic agents for the treatment of cancer [22–26]. PDK1 also plays a major role in downstream signaling of the proteins in this pathway [27–30]. The discovery of dibenzo[c,f][2,7]naphthyridines and 8,9-dimethoxy-5-(2-aminoalkoxy-pyridin-3-yl)-benzo[c][2,7]naphthyridin-4-ylamines as potent and selective PDK1 inhibitors inspired us to work on 10-methoxy dibenzo[b,h][1,6]naphthyridine derivatives. Due to the significance of dibenzo[b,h][1,6]naphthyridines in biology, scarcity of the number of literatures, and in continuation of our research interest in this scaffold, the present work is carried out. In this work, we described the structure-based design, an efficient way of synthesizing 10-methoxy dibenzo[b,h][1,6]naphthyridine-2-substituted carboxamides, their cytotoxic activity against A549 and normal Vero cell lines, and the molecular docking investigations.

## Materials and methods

### Chemistry

All the chemicals used in the study are of commercially available high-purity grade (Aldrich or Merck, India). The solvents were of reagent grade and used as supplied commercially. The melting point was determined using an open-ended capillary tube on Buchi Melting point B-540 instrument. IR spectra were recorded with KBr pellets on a Bruker Alpha-E spectrometer. <sup>1</sup>H NMR spectra (300 or 400 MHz) were recorded for (DMSO-d<sub>6</sub>/CDCl<sub>3</sub>) solutions on Bruker 300-Ultra Shield spectrometer. <sup>1</sup>H NMR data are reported as follows: chemical shift (multiplicity (s = singlet, d = doublet, t = triplet, m = multiplet, dd = doublet of the doublet, and br s = broad singlet), coupling constant (*J*), integrations, and assignment). Coupling constant *J* values are given in Hz. Electrospray ion mass spectra (*m/z*) were recorded using LC/MSD TRAP XCT Plus (1200 Agilent).

### Synthesis procedure

#### Ethyl-4-(((2-chloro-7-methoxyquinolin-3-yl)methylene)amino)benzoate

2-chloro-7-methoxyquinoline-3-carbaldehyde (**3**) was prepared as per the literature procedure [31]. To the stirred

solution of 2-chloro-7-methoxyquinoline-3-carbaldehyde (100.4 g, 0.45 mol, 1.0 eq) in ethanol (1.0 L, 10 v), we slowly added acetic acid (38.9 ml, 0.67 mol, 1.5 eq) and 4-amino ethyl benzoate (74.86 g, 0.45 mol, 1.0 eq) at 0–5 °C. We raised the reaction mass temperature to ambient temperature and stirred for 12 h. After completion of the reaction (by TLC), the solid was filtered and washed with ethanol to obtain yellow solid in 70% yield. <sup>1</sup>H NMR (400 MHz, DMSO-d<sub>6</sub>, δ ppm): 1.34 (t, 3H, *J* = 7.2 Hz, CH<sub>3</sub>), 3.97 (s, 3H, OCH<sub>3</sub>), 4.34–4.32 (m, 2H, CH<sub>2</sub> ethyl group), 7.44–7.36 (m, 4H, aromatic H), 8.04 (d, 2H, *J* = 8.4 Hz, aromatic H), 8.18 (d, 1H, *J* = 9.2 Hz, aromatic H), 8.90 (s, 1H, aromatic H), and 9.12 (s, 1H, imine H). Anal. calcd for C<sub>20</sub>H<sub>17</sub>ClN<sub>2</sub>O<sub>3</sub>: C, 65.13; H, 4.65; N, 7.60; found: C, 65.25; H, 4.82; N, 7.58%.

#### Ethyl-4-(((2-chloro-7-methoxyquinolin-3-yl)methyl)amino)benzoate

To the stirred solution of ethyl-4-[(2-chloro-7-methoxyquinolin-3-yl)methylene]amino}benzoate (148.0 g, 0.40 mol, 1.0 eq) in ethanol (2.0 L, 14 v), we slowly added sodium borohydride (30.3 g, 0.80, 2.0 eq) at 0–5 °C. We raised the reaction mass temperature to ambient temperature and stirred for 8 h. After completion of the reaction (by TLC), the solid was filtered and washed with methanol to obtain yellow solid in 80% yield. MP: 138.1–145.0 °C. <sup>1</sup>H NMR (300 MHz, DMSO-d<sub>6</sub>, δ ppm): 1.25 (t, 3H, *J* = 7.2 Hz, CH<sub>3</sub>), 3.91 (s, 3H, OCH<sub>3</sub>), 4.16–4.22 (q, 2H, *J* = 7.2 Hz, CH<sub>2</sub> ethyl group), 4.49 (s, 2H, CH<sub>2</sub>), 6.66 (d, 2H, *J* = 8.8 Hz, aromatic H), 7.17–7.27 (m, 2H, aromatic H), 7.37 (s, 1H, aromatic H), 7.70 (d, 2H, *J* = 8.4 Hz, aromatic H), 7.89 (d, 1H, *J* = 9.2 Hz, aromatic H), and 8.19 (s, 1H, aromatic H); IR (KBR, ν cm<sup>-1</sup>): 3378, 2978, 1619, 1600, 1582, 1280, 1176, and 1112; LCMS (ESI) *m/z* 371.8 Da [M + H]<sup>+</sup>. Anal. calcd for C<sub>20</sub>H<sub>19</sub>ClN<sub>2</sub>O<sub>3</sub>: C, 64.78; H, 5.16; N, 7.55; found: C, 64.70; H, 5.20; N, 7.59%.

#### Ethyl-10-methoxy dibenzo[b,h][1,6]naphthyridine-2-carboxylate

To the stirred solution of ethyl-4-[(2-chloro-7-methoxyquinolin-3-yl)methyl]amino}benzoate in dimethylacetamide (5 v), palladium acetate (0.1 eq), tri-tert-butylphosphine tetrafluoroborate (0.15 eq), and potassium carbonate (1.5 eq) were added at ambient temperature. Then we raised the reaction mass temperature to 140–150 °C and stirred for 4 h. After completion of the reaction (by TLC), the reaction mass was cooled to ambient temperature. The reaction mass was filtered with celite bed and washed with dichloromethane (5 v). The reaction mass was extracted with dichloromethane (10 v) and washed with water (2 × 4 v), brain solution (4 v), and then dried over

anhydrous sodium sulfate and concentrated the organic layer completely to get crude. The crude was subjected to column chromatography to obtain the desired pure product as yellow-color solid in 30% yield. MP: 185.4–190.7 °C. <sup>1</sup>H NMR (400 MHz, DMSO-d<sub>6</sub>, δ ppm): 1.53 (t, 3H, *J* = 7.2 Hz, CH<sub>3</sub>), 4.11 (s, 3H, OCH<sub>3</sub>), 4.51–4.57 (q, 2H, *J* = 7.2 Hz, CH<sub>2</sub> ethyl group), 7.35–7.38 (m, 1H, aromatic H), 7.72 (d, 1H, aromatic H), 8.02 (d, 1H, *J* = 8.4 Hz, aromatic H), 8.23 (d, 2H, *J* = 8.4 Hz, aromatic H), 8.47–8.50 (m, 1H, aromatic H), 8.80 (s, 1H, aromatic H), 9.40 (s, 1H, aromatic H), and 9.99 (d, 1H, aromatic H); <sup>13</sup>C NMR (100 MHz, DMSO-d<sub>6</sub>, δ ppm) δ: 14.3 (CH<sub>3</sub>), 56.0 (OCH<sub>3</sub>), 61.2 (OCH<sub>2</sub>), 106.2 (aromatic C), 118.2 (aromatic C), 121.5 (aromatic C), 122.9 (aromatic C), 124.3 (aromatic C), 125.5 (aromatic C), 128.2 (aromatic C), 129.8 (aromatic C), 130.2 (aromatic C), 130.7 (aromatic C), 138.3 (aromatic C), 146.9 (aromatic C), 148.3 (aromatic C), 152.0 (aromatic C), 157.0 (aromatic C), 163.1 (aromatic C), and 165.5 (COO); IR (KBR, ν cm<sup>-1</sup>): 2924, 2853, 1705, 1599, 1418, 1299, 1228, and 1116; LCMS (ESI) *m/z*: 333.7 Da [M + H]<sup>+</sup>. Anal. calcd for C<sub>20</sub>H<sub>16</sub>N<sub>2</sub>O: C, 72.28; H, 4.85; N, 8.43; found: C, 72.35; H, 4.91; N, 8.45%.

### 10-methoxy dibenzo[b,h][1,6]naphthyridine-2-carboxylic acid

To the stirred solution of ethyl-10-methoxy dibenzo[b,h][1,6]naphthyridine-2-carboxylate in tetrahydrofuran (7 v), lithium hydroxide solution ((2.0 eq) in water (3.0 v)) was added at ambient temperature. Then we raised the reaction mass temperature to 95–100 °C and stirred for 8 h. After completion of the reaction (by TLC), the reaction mass was cooled to ambient temperature and concentrated THF to get a thick syrup. The reaction mass was extracted with dichloromethane (10 v) and washed with water (2 × 4 v), brain solution (4 v), and then dried over anhydrous sodium sulfate and concentrated the organic layer completely to get the desired product as yellow solid in 62% yield, MP: 201.5–210.3 °C. <sup>1</sup>H NMR (400 MHz, DMSO-d<sub>6</sub>, δ ppm): 4.06 (s, 3H, OCH<sub>3</sub>), 7.44 (dd, 1H, *J*<sub>1</sub> = 8.6 Hz, *J*<sub>2</sub> = 2.4 Hz, aromatic H), 7.75 (s, 1H, aromatic H), 8.21–8.27 (m, 2H, aromatic H), 8.70 (dd, 1H, *J*<sub>1</sub> = 8.4 Hz, *J*<sub>2</sub> = 2.0 Hz, 1H, aromatic H), 9.28 (s, 1H, aromatic H), 9.56 (s, 1H, aromatic H), 9.80 (s, 1H, aromatic H), and 13.34 (s, 1H, COOH); <sup>13</sup>C NMR (100 MHz, DMSO-d<sub>6</sub>, δ ppm) δ: 56.0 (OCH<sub>3</sub>), 106.2 (aromatic C), 118.1 (aromatic C), 121.4 (aromatic C), 123.0 (aromatic C), 124.2 (aromatic C), 126.0 (aromatic C), 129.1 (aromatic C), 129.5 (aromatic C), 130.5 (aromatic C), 130.7 (aromatic C), 138.1 (aromatic C), 147.0 (aromatic C), 148.1 (aromatic C), 152.0 (aromatic C), 156.7 (aromatic C), 163.0 (aromatic C), and 167.0 (COOH); IR (KBR, ν cm<sup>-1</sup>): 3408, 2924, 2352, 1915, 1599, 1438, 1231, 1164, and 848; LCMS (ESI) *m/z*: 305.7 Da [M + H]<sup>+</sup>. Anal. calcd for C<sub>18</sub>H<sub>12</sub>N<sub>2</sub>O<sub>3</sub>:

C, 71.05; H, 3.97; N, 9.21; found: C, 71.12; H, 4.20; N, 9.19%.

### Structure-based design

Structure-based drug design is the most powerful tool when it is a part of an entire drug lead discovery process [32]. Energy-based pharmacophore has been utilized as a good starting point for the design of inhibitors of many disease targets [33–35]. It is anticipated that we could synthesize any biologically specific molecule with the use of epharmacophoric approach instead of rational synthesis. For this purpose, the three-dimensional coordinates for the cocrystallized structure of PDK1 and the dibenzonaphthyridine inhibitor were downloaded from Protein Data Bank (<https://doi.org/10.2210/pdb2R7B/pdb>). Epharmacophore utility in Phase in Schrodinger suite was used to develop a pharmacophore model. A model hypothesis was created utilizing the receptor cavity and by defining its binding site with important amino acid residues that are involved in hydrogen bonds with all the other cocrystallized inhibitors in protein data bank. A model hypothesis with donors as projected points, including the exclusion spheres, was created by keeping all the other parameters as default. The developed pharmacophore was validated as good using decoys and actives. A mini library of 44 compounds was enumerated with the available simple fragments in the Schrodinger database by custom R-group enumeration. The developed pharmacophore was screened against these compounds, and the hits are validated by the fitness scores.

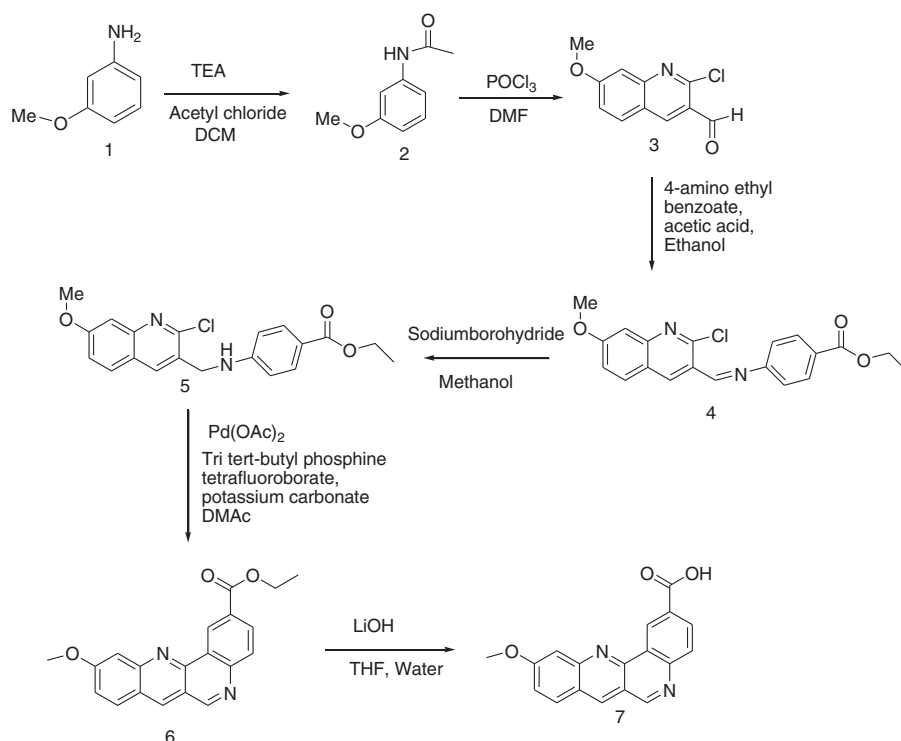
### General procedure for the synthesis of 10-methoxy dibenzo [b,h][1,6]naphthyridine-2-substituted carboxamide derivatives (8a–i)

To the stirred solution of 10-methoxy dibenzo [b,h][1,6]naphthyridine-2-carboxylic acid (200 mg) in tetrahydrofuran (4.0 mL, 20 v), hydroxybenzotriazole (1.3 eq), EDC HCl (2.0 eq), and amine (2.0 eq) were added at ambient temperature and stirred for 24 h. After completion of the reaction (by TLC), it resulted in a concentrated THF to get a thick syrup. The reaction mass was extracted with dichloromethane (100 mL) and washed with water (2 × 400 mL), brain solution (400 mL), and then dried over anhydrous sodium sulfate and concentrated the organic layer completely to get the crude product. The crude was subjected to column chromatography to obtain the desired pure products as yellow solids.

### Biological evaluation

In order to determine the antiproliferative activity of the synthesized compounds, MTT assay against A549 cancer

**Scheme 1** Synthesis of 10-methoxy dibenzo[b,h][1,6]naphthyridine-2-carboxylic acid



cells and normal Vero cell lines was carried out. The cells were incubated with the test compounds at a wide concentration range of picomolar to millimolar. Both the A549 (human lung carcinoma cell line) and Vero (African Green Monkey kidney cell lines) cells were cultured in DMEM medium supplemented with 10% fetal bovine serum at 37 °C with 5% CO<sub>2</sub>. The cell viability upon different compound treatments was evaluated in both the cells by MTT (3-[4,5-methylthiazol-2-yl]-2,5-diphenyl-tetrazolium bromide).

Pemetrexed, a clinical antitumor drug, was used as a marker to evaluate the relative cytotoxic efficiency of synthesized compounds. The percentage of cell viability was calculated by the ratio of the difference in the OD values obtained from wells carrying cells treated with compounds and the blank wells versus the difference in the OD values obtained in negative and the blank wells. The IC<sub>50</sub> values (the concentration that inhibited cell viability to 50% of the control) were determined by nonlinear regression method.

## Computational

The molecular docking studies were carried out to validate the specific binding pattern of the designed ligands. The contribution of different types of interactions and their correlation with the similar compounds are expected. The computation was carried out using the Schrödinger molecular modeling software package. Docking was performed by using the Glide integrated with Maestro (Schrödinger,

LLC [36]) interface on the windows operating system. Absorption, distribution, metabolism, and excretion (ADME) profile together with binding affinity and selectivity toward the target leads to the discovery of innovative scaffolds in drug design. Chemical entities with such pharmacological profile will reach the success in the drug development process. All the synthesized ligands are neutralized and checked for their ADME properties using QIKPROP [36], and some of the parameters were calculated by SwissADME [37].

## Results and discussion

### Structure-based design

As our research interest is on dibenzonaphthyridine scaffold, the synthesis route starting from 3-methoxyaniline by using easily available reagents was first identified to get 10-methoxy dibenzo[b,h][1,6]naphthyridine carboxylic acid as given in Scheme 1.

In order to proceed to the synthesis step for further useful bioactive compounds, the literature search was carried out. It was found that the protein–ligand complex crystal structure deposited in protein data bank (PDB Id: 2R7B) has the cocrystallized dibenzonaphthyridine inhibitor [10] (Fig. 1a). Furthermore, due to its structural similarity, it is anticipated that the structure–activity relationship of newly synthesized two substituted 10-methoxy dibenzo[b,h][1,6]

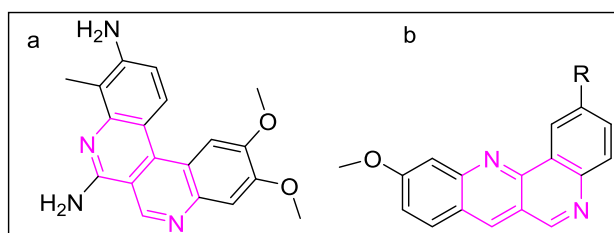


**Fig. 1** **a** 10,11-dimethoxy-4-methyldibenzo[*c,f*]-2,7-naphthyridine-3,6-diamine. **b** 10-methoxy dibenzo [b,h][1,6]naphthyridine-2-substituted carboxamide scaffold

naphthyridine derivatives will be similar. All the ligands, which are in the crystallized structures of PDK1, were further analyzed for the interacting residues (Table S1). It was found that the residues Leu88, Ser92, Ser94, Val96, Lys111, Glu130, Ser160, Ala162, Lys163, Glu166, Glu209, Asn210, Thr222, and Asp223 involved in hydrogen bonds with the cocrystallized ligands. A structure-based pharmacophore model was developed using the receptor cavity and the binding-site residues involved in hydrogen bonding mentioned above in epharmacophore approach in Schrödinger suite of programs.

The developed epharmacophore was validated using decoys and actives, and it successfully predicted the most active compound with acceptable fitness scores of  $>0.7$ . The hypothetical model consists of seven site features of type ANNRRRD and each of them contributed to hydrogen bonds in most of the structures with the amino acid residues in the active site of PDK1. The exclusion spheres were also taken into account while screening. In the quest of determining which functional groups to be attached, a mini library is developed by having the central core as 10-methoxy dibenzo[b,h][1,6]naphthyridine and varying the attachments in position 2 by simple substituents (Fig. 1b). A series of 44 compounds were enumerated with the available simple reagents in the software database. The developed epharmacophore along with the exclusion spheres was screened against these 44 compounds, and it was found that morpholine and carboxamide analogs as the topmost hits with fitness score  $>1$  (Table S2) and hence the carboxamide series was planned initially for synthesis. The alignment of a developed pharmacophore with a carboxamide derivative with four-point matches out of seven can be viewed from Fig. 2.

### Synthesis of 10-methoxy dibenzo[b,h][1,6]naphthyridine-2-substituted carboxamide derivatives (8a–i)

Synthesis of 10-methoxy dibenzo [b,h][1,6]naphthyridine-2-substituted carboxamide derivatives was carried out as per Scheme 1. Synthesis was carried out with acetylation of

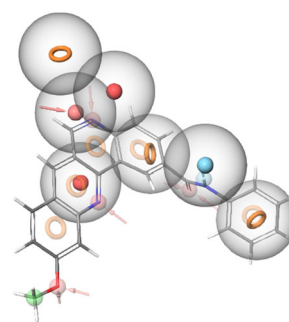


**Fig. 2** Pharmacophore alignment with carboxamide derivative with matching four points of site feature ADRR

3-methoxyaniline followed by Vilsmeier–Haack reaction using DMF–POCl<sub>3</sub> as reported [31] to afford 2-chloro-7-methoxyquinoline-3-carbaldehyde (**3**). The aldehyde **3** obtained was converted into imine **4** with 4-amino ethyl benzoate using acid media, which was then reduced to amine **5** using sodium borohydride.

We targeted to synthesize ethyl-10-methoxy dibenzo[b, h][1,6] naphthyridine-2-carboxylate **6** from intermediate **5** by intramolecular cyclization/annulation of C–H arylation to provide ethyl-10-methoxy-5,6-dihydrodibenzo[b,h][1,6] naphthyridine-2-carboxylate, which subsequently underwent aerial oxidation to provide the desired compound. Initially, we have tried the reaction using palladium chloride and sodium acetate condition as reported [38] and found no desired product formation. This may be due to the presence of ester functional group in the aryl system, which might be having either less reactivity or the ester group hydrolyzed/decomposed at a higher temperature of 130 °C in dimethylacetamide, which would have led to the undesired product. Furthermore, several attempts were made to synthesize intermediate **6** by using different types of palladium catalysts and ligands. Finally, we were successful in synthesizing the desired product **6** by using palladium acetate as a catalyst and tri-*tert*-butylphosphine tetrafluoroborate as a ligand in the presence of potassium carbonate in dimethylacetamide. During this reaction, palladium(0) might be chelating with the aryl system and aniline nitrogen to form a five-membered system that resulted in the oxidative addition of aryl chloride to form Pd (II) followed by reductive elimination of H–Pd–Cl to give six-membered ethyl-10-methoxy-5,6-dihydrodibenzo[b,h][1,6]naphthyridine-2-carboxylate. The resultant material would have undergone aerial oxidation to attain the more stable extended conjugative aromatic system. We have not observed any side-product biaryl impurity in the reaction, which would have come from intermolecular reaction; hence, the major desired product **6** supports that this reaction works through intramolecular C–H annulation.

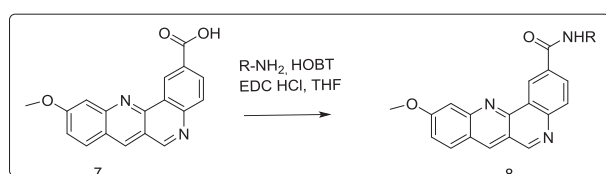
10-methoxy-dibenzonaphthyridine-2-carboxylate **6** synthesized above was then hydrolyzed to acid and subjected to

amide preparation using various aliphatic amines and substituted benzyl amines to afford a novel series of compounds as shown in Scheme 2. The newly synthesized compounds were characterized by elemental analysis, and  $^1\text{H}$  NMR,  $^{13}\text{C}$  NMR, IR, and mass spectrometry. The detailed synthetic procedures and the respective spectral data are given in Supplementary information.

## Molecular docking

The three-dimensional crystal structure of human PDK1 crystallized with dibenzo[*c,f*][2,7]naphthyridine was obtained from protein data bank (PDB Id: 2R7B). The structure was prepared by deleting the cofactors, ligands, and the crystallographically observed water molecules, and refined using OPLS2005 force field in Prime. The active site of the protein was defined by the centroid of all interacted residues in the other observed PDK1 complex structures in PDB to generate the grid. The ligand coordinates were obtained by their 2D structures and energy minimized with OPLS2005. The induced-fit docking calculations were carried out. The redocking of the crystallized complex was done initially by extracting the ligand coordinates of the complexed structure, and the docking algorithm resulted in exactly the same type of interactions as in the crystal structure. The induced-fit docking of the test compounds afforded the better scores ranging from  $-8.08$  to  $-10.446$  kcal/mol. Among all, **8b**, **8g**, and **8h** have comparable glide scores, indicating that these compounds might possess similar binding affinity with the target protein PDK1.

The molecular docking results of the highly scored compounds **8b**, **8d**, **8f**, **8g**, and **8h** demonstrated the



**Scheme 2** Synthesis of 2-substituted carboxamides

hydrogen-bonded interactions with Lys111, Ala162, and Glu166 (Table 1). Also, the gatekeeper residue Ala159 was in hydrophobic contact with all the compounds, except **8c**. The dibenzonaphthyridine ring sits well in the hydrophobic region at the ATP-binding site (Fig. S2), and the substituent  $\text{OCH}_3$  demonstrated the hydrogen-bonded interactions with Lys111. It was found that the carboxamide group was clearly recognized with both nitrogen and oxygen atoms at important contacts with Leu88 and Glu166, respectively. Thus, the planarity of the heterocycles is responsible for positioning the molecule at the hinge region, as well as interactions with an important amino acid residue Ala162, as similar to dibenzonaphthyridine from the crystallized complex. The carboxamide substituent is responsible for the interactions with leu88 and Glu166. These results of molecular docking can be used to further detail to which amino acid residue the cellular active compounds might interact, and to what extent to inhibit the PDK1 and in developing potent inhibitors.

## MTT assay

The synthesized compounds were evaluated for cytotoxicity against A549 (a non-small-cell lung cancer line) and Vero (African kidney normal cell line) by MTT assay with Pemetrexed as positive control, and the inhibition results are interpreted in terms of  $\text{IC}_{50}$  values. The expression pathways in A549 include PI3K/AKT/mTOR, MAPK, NF- $\kappa\text{B}$ , etc., in which PDK1 expression was reported as 14.7 TPM and mTOR in 22.8 TPM [39, 40]. PDK1 downstream the PI3K cell-signaling pathways in cells was reported to be highly expressed in different lung cancer cell lines in addition to many breast cancer cells [39, 41]. As A549 lung cancer cell lines were widely studied and also have good PDK1 expression terms, it was chosen for the present study. Pemetrexed, a lung cancer drug [42], was used as a positive control. The inhibitory efficiency of the compounds was assayed after 24 h of incubation of the cells in drug-containing medium at a concentration range of  $10^{-12}$ – $10^{-3}$  M (Fig. S1). Significant inhibition of growth was defined as

**Table 1** Induced-fit docking calculations with amino acid residues involved in hydrogen-bonded interactions

Compounds	Glide energy (kcal/mol)	Docking score (kcal/mol)	Interacting residues
<b>8a</b>	$-59.951$	$-9.524$	Leu88, Lys111, Ala162, and Glu166
<b>8b</b>	$-63.483$	$-10.014$	Lys111, Ala162, and Glu166
<b>8c</b>	$-60.530$	$-8.081$	Glu90 and Thr222
<b>8d</b>	$-64.399$	$-10.446$	Leu88, Lys111, Ala162, and Glu166
<b>8e</b>	$-64.081$	$-9.532$	Glu90, Lys111, Ala162, and Glu166
<b>8f</b>	$-57.371$	$-10.310$	Lys111, Ala162, and Glu166
<b>8g</b>	$-54.466$	$-10.078$	Leu88, Lys111, Ala162, and Glu166
<b>8h</b>	$-53.443$	$-10.292$	Lys111, Ala162, and Glu166
<b>8i</b>	$-57.574$	$-9.725$	Leu88, Lys111, Ala162, and Glu166

50% or less of control cell growth. To our expectation, the results are promising in which all the compounds exhibited cytotoxicity against lung cancer cell line and the  $IC_{50}$  of pemetrexed was found to be 1.15  $\mu\text{M}$ . The compounds **8b**, **8e**, and **8i** were found to be much significant with lesser  $IC_{50}$  values (1.0, 1.04, and 19.7  $\mu\text{M}$ , respectively). These results are also correlated with the docking output wherein the docking scores for **8b** and **8e** are high. On the basis of antiproliferative screening, the preliminary structure–activity relationship study suggested that fluorine substituent at the second position of the aromatic ring attached to carboxamide might be responsible for the enhanced activity of the compounds. This can be further explained by the presence of a chlorosubstituent at the second position in compound **8a** that possess a higher  $IC_{50}$  value of 15  $\mu\text{M}$  when compared to **8b** and **8e**. Thus, the compounds with highly electron-withdrawing groups at the second position of the phenyl ring are more potent. The steric hindrance offered by the bulky  $\text{CF}_3$  group at ortho position of the fluorine-substituted phenyl ring may be the cause of decreasing the activity of the compound in **8c** ( $IC_{50} = 37.4 \mu\text{M}$ ), which is similar in the case of **8d** ( $IC_{50} = 43.7 \mu\text{M}$ ). Also, in the case of aliphatic amides, the longer aliphatic chain and the bulkiness of N-dimethyl in **8i** ( $IC_{50} = 19.7 \mu\text{M}$ ) make the compound free to rotate at that end and hence decrease the chance of binding with biomolecules in the cell. This might be attributed to a slight decrease in its activity. In the case of **8g** and **8h**, the short chain with the methyl group can be flipped in any direction to interact with other molecules, and is similar to the fixed planar phenyl ring of **8b** and **8e**. The mechanism of cytotoxicity includes DNA intercalation, signaling arrest, or others, and this study served as a preliminary screen for the hit generation. All the three compounds that are active against A549 cells are found to possess docking scores close to  $-10.0 \text{ kcal/mol}$  and complex energies ranging from  $-57$  to  $-63 \text{ kcal/mol}$  with four to five intermolecular hydrogen bonds (Fig. S3).

In drug design and development, the major challenge is to obtain the compounds with selectivity toward the cancer cells compared to normal cells. Hence, the cytotoxicity study of all the compounds with normal cells was also carried out (Fig. S2). The cell death of normal cells occurs only at larger concentrations of the compounds when compared to cancer cell lines, and thus, the tested compounds, particularly **8b** and **8e**, are selective toward the cancerous cell lines when compared to Pemetrexed that is toxic to cells only at higher concentrations.

### In silico ADME predictions

The most important pharmacological parameters in ADME were predicted by SwissADME powered by chemaxon

algorithm and by QikProp in maestro. All the active compounds were found to be 100% effective for human oral absorption, which is a desirable fact. None of the compounds have violated the Lipinski's rule of five, as well as logP, human serum albumin binding, blood–brain–barrier penetration, donor, and acceptor HB were within the range indicating the drug-like behavior of compounds. The lipophilicity (XlogP3), solubility (log S), and the other drug-likeness parameters were found to be in acceptable range with the other marketed drugs (Table S3). QPPCaco, a cell-permeability key factor that describes the drug metabolism, ranged from 388 to 2106. As this is a target-oriented synthesis, the target requires significant hydrophobic interactions with the inhibiting compounds, and hence some of the compounds might have suboptimal physicochemical profiles that can be improved by further modifications.

### Conclusion

In summary, we have successfully synthesized and characterized 10-methoxy dibenzo[b,h][1,6]naphthyridine carboxylic acid of biological interest. The inhibitors of PDK1 based on this scaffold were designed by epharmacophoric approach. The screening of a simple library of substituted 10-methoxy dibenzo[b,h][1,6]naphthyridine carboxylic acid derivatives against the developed epharmacophore was carried out. Based on the top hits, a series of novel 10-methoxy dibenzo[b,h][1,6]naphthyridine-2-substituted carboxamide derivatives was synthesized and characterized. These compounds exhibited anticancer activity against A549 cancer cell line. The potent compounds were further evaluated with normal cell lines (Vero) and exhibited selectivity toward cancerous cells. The molecular docking studies were conducted, and the binding site and interactions were modeled for the compounds **8a–8i**. **8b** and **8e** were reported to be the best active compound against A549 cells, which will not affect the normal cells when compared to Pemetrexed. These results also provide understanding for further pharmacophoric modifications for the design of potent and selective inhibitors for PDK1 based on dibenzonaphthyridine scaffold.

**Acknowledgements** The author KNV is highly thankful to the Department of Science and Technology, New Delhi for financial support under WOS-A Scheme (SR/WOS-A/CS-1084/2014). KNV also acknowledges the computational facility and Schrödinger access offered by Prof. D. Velmurugan, BSR Faculty, Center for crystallography and Biophysics, University of Madras, Chennai.

### Compliance with ethical standards

**Conflict of interest** The authors declare that they have no conflict of interest.

**Publisher's note** Springer Nature remains neutral with regard to jurisdictional claims in published maps and institutional affiliations.

## References

- Leisher GY, Froelich EJ, Gruett MD, Bailey JH, Brundage P. Communication to the editor. *J Med Chem.* 1962;5:1063–5. <https://doi.org/10.1021/jm01240a021>.
- Feng BB, Lu L, Li C, Wang XS. Iodine-catalyzed synthesis of dibenzo[b,h][1,6]naphthyridine-11-carboxamides via a domino reaction involving double elimination of hydrogen bromide. *Org Biomol Chem.* 2016;14:2774–9. <https://doi.org/10.1039/c5ob02620b>.
- Eweas AF, Khalifa NM, Ismail NS, Al-Omar MA, Soliman AM. Synthesis, molecular docking of novel 1,8-naphthyridine derivatives and their cytotoxic activity against HepG2 cell lines. *Med Chem Res.* 2014;23:76–86. <https://doi.org/10.1007/s00044-013-0604-6>.
- Zeng LF, Wang Y, Kazemi R, Xu S, Xu ZL, Sanchez TW, et al. Repositioning HIV-1 integrase inhibitors for cancer therapeutics: 1,6-naphthyridine-7-carboxamide as a promising scaffold with drug-like properties. *J Med Chem.* 2012;55:9492–509. <https://doi.org/10.1021/jm300667v>.
- Bedard J, May S, L'Heureux L, Stamminger T, Copsey A, Drach J. Antiviral properties of a series of 1,6-naphthyridine and 7, 8-dihydroisoquinoline derivatives exhibiting potent activity against human cytomegalovirus. *Antimicrob Agents Chemother.* 2000;44:929–37.
- Hassaneen HM, Wardkhan WW, Mohammed YS. A novel route to isoquinoline[2,1-g][1,6]naphthyridine, pyrazolo[5,1-a]isoquinoline and pyridazino[4',5':3,4]pyrazolo[5,1-a]isoquinoline derivatives with evaluation of antitumor activities. *Z Naturforsch.* 2013;68:895–904. <https://doi.org/10.5560/znb.2013-3101>.
- Kumar A, Kumar A, Gupta RK, Paitandi RP, Singh KB, Trigun SK, et al. Cationic Ru(II), Rh(III) and Ir(III) complexes containing cyclic  $\pi$ -perimeter and 2-aminophenyl benzimidazole ligands: synthesis, molecular structure, DNA and protein binding, cytotoxicity and anticancer activity. *J Organomet Chem.* 2016;801:68–79. <https://doi.org/10.1016/j.jorganchem.2015.10.008>.
- Prabha K, Rajendra Prasad KJ. Benzoquinoline amines—key intermediates for the synthesis of angular and linear dinaphtho-naphthyridines. *J Adv Res.* 2015;6:631–41. <https://doi.org/10.1016/J.JARE.2014.02.007>.
- Vennila KN, Prabha K, Manoj M, Prasad KJ, Velmurugan D. 2-Chloro-7-methyl-12-phenyldibenzo[b,g][1,8]naphthyridin-11 (6H)-one. *Acta Crystallogr Sect E Struct Rep. Online.* 2010;66: o1823. <https://doi.org/10.1107/S160053681002430X>.
- Gopalsamy A, Shi M, Boschelli DH, Williamson R, Olland A, Hu Y, et al. Discovery of dibenzo[c,f][2,7]naphthyridines as potent and selective 3-phosphoinositide-dependent kinase-1 inhibitors. *J Med Chem.* 2007;50:5547–9. <https://doi.org/10.1021/jm070851i>.
- Nittoli T, Dushin RG, Ingalls C, Cheung K, Floyd MB, Fraser H, et al. The identification of 8,9-dimethoxy-5-(2-aminoalkoxy-pyridin-3-yl)-benzo[c][2,7]naphthyridin-4-ylamines as potent inhibitors of 3-phosphoinositide-dependent kinase-1 (PDK-1). *Eur J Med Chem.* 2010;45:1379–86. <https://doi.org/10.1016/j.ejmech.2009.12.036>.
- Ruchelman AL, Singh SK, Ray A, Wu XH, Yang JM, Li TK, et al. 5H-Dibenzo[c,h]1,6-naphthyridin-6-ones: novel topoisomerase I-targeting anticancer agents with potent cytotoxic activity. *Bioorg Med Chem.* 2003;11:2061–73. [https://doi.org/10.1016/S0968-0896\(03\)00051-8](https://doi.org/10.1016/S0968-0896(03)00051-8).
- Reha D, Kabelác M, Ryjáček F, Sponer J, Sponer JE, Elstner M, et al. Intercalators. 1. Nature of stacking interactions between intercalators (ethidium, daunomycin, ellipticine, and 4',6-diaminide-2-phenylindole) and DNA base pairs. Ab initio quantum chemical, density functional theory, and empirical potential study. *J Am Chem Soc.* 2002;124:3366–76.
- Kiselev E, Dexheimer TS, Pommier Y, Cushman M. Design, synthesis, and evaluation of dibenzo[c,h][1,6]naphthyridines as topoisomerase I inhibitors and potential anticancer agents. *J Med Chem.* 2010;53:8716–26. <https://doi.org/10.1021/jm101048k>.
- Liu Q, Wang J, Kang SA, Thoreen CC, Hur W, Ahmed T, et al. Discovery of 9-(6-aminopyridin-3-yl)-1-(3-(trifluoromethyl)phenyl)benzo[h][1,6]naphthyridin-2(1H)-one (Torin2) as a potent, selective and orally available mTOR inhibitor for treatment of cancer. *J Med Chem.* 2011;54:1473–80. <https://doi.org/10.1021/jm101520v>. Discovery.
- Okuma K, Koga T, Ozaki S, Suzuki Y, Horigami K, Nagahora N, et al. One-pot synthesis of dibenzo[b,h][1,6]naphthyridines from 2-acetylaminobenzaldehyde: application to a fluorescent DNA-binding compound. *Chem Commun.* 2014;50:15525–8. <https://doi.org/10.1039/c4cc07807a>.
- Okuma K, Oba A, Kuramoto R, Iwashita H. Synthesis and fluorescence properties of 1, 1-dimethyl-1, 4- dihydrodibenzo [b, h][1, 6] naphthyridinium Iodides: turn-on type detection of DNA. 2017:6885–8. <https://doi.org/10.1002/ejoc.201701277>.
- Tateno K, Ogawa R, Sakamoto R, Tsuchiya M, Kutsumura N, Otani T, et al. Dibenzopyrrolo[1,2-a][1,8]naphthyridines: synthesis and structural modification of fluorescent L-shaped heteroarenes. *J Org Chem.* 2018;83:690–702. <https://doi.org/10.1021/acs.joc.7b02674>.
- Kumar R, Asthana M, Singh RM. Pd-catalyzed one-Pot stepwise synthesis of benzo[b][1,6]naphthyridines from 2-chloroquinoline-3-carbonitriles using sulfur and amines as nucleophiles. *J Org Chem.* 2017;82:11531–42. <https://doi.org/10.1021/acs.joc.7b02147>.
- Muthukrishnan I, Vinoth P, Vivekanand T, Nagarajan S, Uma Maheswari C, Menéndez JC, et al. Synthesis of 5,6-dihydrodibenzo[b,h][1,6]naphthyridines via copper bromide catalyzed intramolecular [4 + 2] hetero-diels-alder reactions. *J Org Chem.* 2016;81:1116–24. <https://doi.org/10.1021/acs.joc.5b02669>.
- Singh JB, Chandra Bharadwaj K, Gupta T, Singh RM. Ligand-free palladium-catalyzed facile construction of tetra cyclic dibenzo [b,h][1,6]naphthyridine derivatives: domino sequence of intramolecular C-H bond arylation and oxidation reactions. *RSC Adv.* 2016;26993–9. <https://doi.org/10.1039/c6ra00505e>.
- Kawade VS. Therapeutic potential of PI3K/Akt/mTOR signalling pathway: effective combination therapy for cancer. *Indian. J Pharm Sci.* 2018;80:702–8.
- Liu P, Cheng H, Roberts TM, Zhao JJ. Targeting the phosphoinositide 3-kinase pathway in cancer. *Nat Rev Drug Discov* 2009;8:627–44.
- Bai X, Li P, Xie Y, Guo C, Sun Y, Xu Q, Zhao D. Overexpression of 3-phosphoinositide-dependent protein kinase-1 is associated with prognosis of gastric carcinoma. *Tumor Biol.* 2016;37:2333–9. <https://doi.org/10.1007/s13277-015-4024-8>.
- Rehan M, Bajouh OS. Virtual screening of naphthoquinone analogs for potent inhibitors against the cancer-signaling PI3K/AKT/mTOR pathway. *J Cell Biol.* 2018;1:12. <https://doi.org/10.1002/jcb.27100>.
- Zhao H, Chen G, Ye L, Yu H, Li S, Jiang WG. DOK7V1 influences the malignant phenotype of lung cancer cells through PI3K/AKT/mTOR and FAK/paxillin signaling pathways. *Int J Oncol.* 2018;381–9. <https://doi.org/10.3892/ijo.2018.4624>.
- Alessi DR, Deak M, Casamayor A, Caudwell FB, Morrice N, Norman DG, et al. 3-Phosphoinositide-dependent protein kinase-1 (PDK1): structural and functional homology with the drosophila DSTPK61 kinase. *Curr Biol.* 1997;7:776–89. [https://doi.org/10.1016/S0960-9822\(06\)00336-8](https://doi.org/10.1016/S0960-9822(06)00336-8).
- Liu Y, Wang J, Wu M, Wan W, Sun R, Yang D, et al. Down-regulation of 3-phosphoinositide-dependent protein kinase-1

- levels inhibits migration and experimental metastasis of human breast cancer cells. *Mol Cancer Res*. 2009;7:944–54. <https://doi.org/10.1158/1541-7786.MCR-08-0368>.
29. Schulze JO, Saladino G, Busschots K, Neimanis S, Süß E, Odadzic D, et al. Bidirectional allosteric communication between the ATP-binding site and theregulatory PIF pocket in PDK1 protein kinase. *Cell Chem Biol*. 2016;23:1193–205. <https://doi.org/10.1016/j.chembiol.2016.06.017>.
  30. Balendran A, Biondi RM, Cheung PC, Casamayor A, Deak M, Alessi DR, et al. A 3-phosphoinositide-dependent protein kinase-1 (PDK1) docking site is required for the phosphorylation of protein kinase C $\zeta$  (PKC $\zeta$ ) and PKC-related kinase 2 by PDK1. *J Biol Chem*. 2000;275:20806–13. <https://doi.org/10.1074/jbc.M000421200>.
  31. Wafaa SH, Mona EI, Ayaa AG, Hanafi HZ. Recent advances in the chemistry of 2-chloroquinoline-3-carbaldehyde and related analogs. *RSC Adv*. 2018;8:8484–515. <https://doi.org/10.1039/C7RA11537G>.
  32. Andricopulo A, Salum L, Abraham D. Structure-based drug design strategies in medicinal chemistry. *Curr Top Med Chem*. 2009;9:771–90. <https://doi.org/10.2174/156802609789207127>.
  33. Natarajan P, Priyadarshini V, Pradhan D, Manne M, Swargam S, Kanipakam H, et al. E-pharmacophore-based virtual screening to identify GSK-3 $\beta$  inhibitors. *J Recept Signal Transduct Res*. 2016;36:445–58. <https://doi.org/10.3109/10799893.2015.1122043>.
  34. Pulla VK, Sriram DS, Viswanadha S, Sriram D, Yogeewari P. Energy-based pharmacophore and three-dimensional quantitative structure–activity relationship (3D-QSAR) modeling combined with virtual screening to identify novel small-molecule inhibitors of silent mating-type information regulation 2 homologue 1 (SIRT1). *J Chem Inf Model*. 2016;56:173–87. <https://doi.org/10.1021/acs.jcim.5b00220>.
  35. Singh KhD, Kirubakaran P, Nagarajan S, Sakkiah S, Muthusamy K, Velmurgan D, et al. Homology modeling, molecular dynamics, e-pharmacophore mapping and docking study of Chikungunya virus nsP2 protease. *J Mol Model*. 2012;39–51. <https://doi.org/10.1007/s00894-011-1018-3>.
  36. Phase, Glide, QikProp, Schrödinger LLC, New York, NY 2015. p. 2017–1.
  37. Daina A, Michielin O, Zoete V. SwissADME: a free web tool to evaluate pharmacokinetics, drug-likeness and medicinal chemistry friendliness of small molecules. *Sci Rep*. 2017;7:1–13. <https://doi.org/10.1038/srep42717>.
  38. Jay Bahadur S, Kishor CB, Tanu G, Radhey MS. Ligand-free palladium-catalyzed facile construction of tetra cyclic dibenzo[b, h][1,6] naphthyridine derivatives: domino sequence of intramolecular C–H bond arylation and oxidation reactions. *RSC Adv*. 2016;6:26993–9.
  39. Khan N, Hadi N, Afaq F, Syed DN, Kweon MH, Mukhtar H. Pomegranate fruit extract inhibits prosurvival pathways in human A549 lung carcinoma cells and tumor growth in athymic nude mice. *Carcinogenesis*. 2007;28:163–73. <https://doi.org/10.1093/carcin/bgl145>.
  40. Korrodi-Gregório L, Soto-Cerrato V, Vitorino R, Fardilha M, Pérez-Tomás R. From proteomic analysis to potential therapeutic targets: functional profile of two lung cancer cell lines, A549 and SW900, widely studied in pre-clinical research. *PLoS ONE*. 2016;11:1–27. <https://doi.org/10.1371/journal.pone.0165973>.
  41. Fyffe C, Falasca M. 3-phosphoinositide-dependent protein kinase-1 as an emerging target in the management of breast cancer. *Cancer Manag Res*. 2013;5:271–80. <https://doi.org/10.2147/CMAR.S35026>.
  42. Cohen MH, Johnson JR, Wang YC, Sridhara R, Pazdur R. FDA drug approval summary: pemetrexed for injection (Alimta) for the treatment of non-small cell lung cancer. *Oncologist*. 2005;10:363–8. <https://doi.org/10.1634/theoncologist.10-6-363>.